


 Cite this: *Chem. Commun.*, 2015, 51, 5414

 Received 7th January 2015,  
 Accepted 6th February 2015

DOI: 10.1039/c5cc00151j

www.rsc.org/chemcomm

# The dramatic effect of the annealing temperature and dielectric functionalization on the electron mobility of indene-C<sub>60</sub> bis-adduct thin films†

 Emanuele Orgiu,<sup>\*a</sup> Marco A. Squillaci,<sup>a</sup> Wassima Rekab,<sup>a</sup> Karl Börjesson,<sup>a</sup> Fabiola Liscio,<sup>b</sup> Lei Zhang<sup>a</sup> and Paolo Samori<sup>\*a</sup>

**Herein we report on the charge transport properties of spin-coated thin films of an n-type fullerene derivative, i.e. the indene-C<sub>60</sub> bis-adduct (ICBA). In particular, the effects of annealing temperature and duration as well as surface functionalization are explored. Electron mobilities approaching 0.1 cm<sup>2</sup> V<sup>-1</sup> s<sup>-1</sup> are reported.**

In the blooming era of flexible electronics, organic thin-film transistors (oTFTs) and solar cells (oSC) have been attracting a great deal of attention as promising candidates for light-weight, large-area and low-cost electronic device applications.<sup>1</sup> Whilst p-type organic semiconductors have been extensively studied, electron transporting semiconductors have been less explored owing to their more pronounced tendency to get their electrical properties altered by environmental oxidants upon exposure to air. However, if organic electronics is to go to the market place, realizing complementary circuits as well as finding valid replacements for electron acceptors in oSC becomes of paramount importance.

Fullerene derivatives including [6,6]phenyl-C<sub>61</sub>-butyric acid methyl ester (PCBM) have been often used as electron transporting materials in oSC<sup>1e,2</sup> and oTFTs.<sup>3</sup> Intensive chemical effort has been put towards the development of fullerene moieties that can be solution-processed, resulting in higher electron mobility with the desired molecular packing. Much of the research on soluble fullerene derivatives therefore focused on diversifying substitution groups and assessing their effects on the electrical performance<sup>2a,4a-c</sup> and air stability.<sup>3c,5</sup> Among all the different derivatives, certainly 1',1'',4',4''-tetrahydro-di[1,4]methanonaphthaleno[1,2:2',3',56,60:2'',3''] [5,6]fullerene-C<sub>60</sub>, also known as the indene-C<sub>60</sub> bis-adduct (ICBA),<sup>6</sup> has garnered a great deal of attention thanks to its promising oSC efficiencies when used in

combination with the hole-transporting poly(3-hexylthiophene) polymer.<sup>2a,b,d,4c,6</sup> Little attention has been paid to the systematic study of ICBA as a single n-type semiconductor component and, to the best of our knowledge, to the effects of both thermal annealing and substrate treatment on the charge transport. Clearly, unraveling the correlation between morphology/structure and the electrical characteristics within ICBA thin films undergoing thermal annealing is a key to understand how electron transport can influence the performances not only of three-terminal devices but also those of organic photovoltaic cells.

Herein we investigate the effects of the annealing temperature and duration of the above-mentioned fullerene molecule and correlate the film morphology to the transport of electrons in thin-film transistors. Further, we explore the effect of the surface energy by water contact angle measurements, and of the annealing conditions on the film morphology by atomic force microscopy. The surface energy is tuned by choosing an appropriate functionalization of the dielectric surface, i.e. SiO<sub>2</sub>, with either hexamethyldisilazane (HMDS) or octadecyltrichlorosilane (OTS). The self-assembled monolayers formed by OTS on thermally-grown SiO<sub>2</sub> lead to a more hydrophobic surface compared to HMDS. The difference in surface energy between OTS- and HMDS-treated SiO<sub>2</sub> affects the interplay between molecule-substrate and molecule-molecule interactions. By modifying such a subtle interaction balance *via* thermal annealing treatments resulted in films featuring field-effect electron mobilities approaching 0.1 cm<sup>2</sup> V<sup>-1</sup> s<sup>-1</sup> which are, to the best of our knowledge, the highest ever reported values for ICBA within the scientific literature.

Transistors in bottom-contact bottom-gate geometry were fabricated on Si-n<sup>++</sup>, acting as a substrate and a gate electrode, with 230 nm thermally-grown SiO<sub>2</sub> (gate dielectric) and pre-patterned interdigitated gold electrodes as the source and drain (Fig. 1). The semiconductor layer was deposited by spin-coating from a 10 mg mL<sup>-1</sup> solution in chloroform in a N<sub>2</sub>-filled glovebox. The films were then annealed in a nitrogen environment for 1 h at 90 °C, 140 °C or 200 °C. A series of films that were not thermally annealed was also explored as reference. Atomic force microscopy

<sup>a</sup> Nanochemistry Laboratory & icFRC, Université de Strasbourg & CNRS, 8 allée Gaspard Monge, 67000, Strasbourg, France. E-mail: orgiu@unistra.fr, samori@unistra.fr

<sup>b</sup> Istituto per la Microelettronica e Microsistemi (IMM) - CNR Bologna, via Gobetti 101, 40129 Bologna, Italy

† Electronic supplementary information (ESI) available: Sample preparation details, atomic force microscopy images, water contact angle, electrical parameter extraction, and structural characterization. See DOI: 10.1039/c5cc00151j



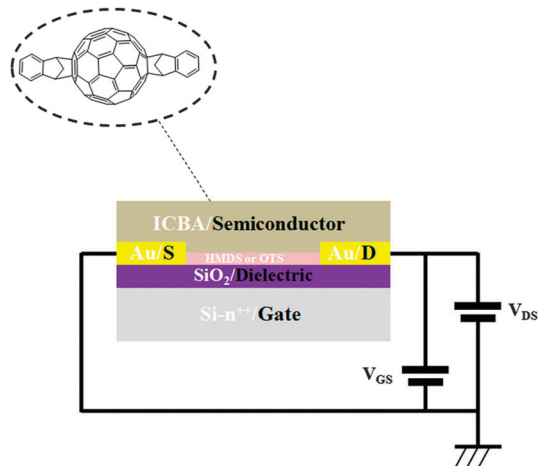


Fig. 1 A bottom-contact bottom-gate transistor with Au gold electrodes. ICBA acts as the active semiconducting layer.

analysis (Fig. 2) revealed that films assembled on HMDS were smoother than those on OTS (see Table S1, ESI<sup>†</sup>). This evidence can be correlated with the larger water contact angle and, therefore, lower surface energy measured on a OTS/SiO<sub>2</sub> vs. HMDS/SiO<sub>2</sub> surface (see ESI<sup>†</sup>). These findings further point to a higher surface affinity of the fullerene derivatives for the HMDS treated SiO<sub>2</sub> surface, in virtue of its relative hydrophilic nature.<sup>7</sup> Hence, the strongest ICBA-HMDS (molecule-substrate) interaction can account for the difference in roughness recorded for films assembled on SiO<sub>2</sub>-treated with either OTS or HMDS, given that in the former case rougher (see Table S1, ESI<sup>†</sup>) and generally taller (see Z-scale) molecular aggregates are formed. Generally, rougher films resulted in lower electron mobilities for OTS vs. HMDS films in the (90–140) °C range and in not-annealed samples. This suggests that on a rougher surface bearing a higher density of molecular aggregates than on HMDS, it is possible that charge transport could be somehow hindered by the presence of a greater amount of grain boundaries. At 200 °C the appearance of films with hollows filled with tall structures is observed for both surface treatments. These tall molecular aggregates ( $Z > 100$  nm) are usually surrounded by bare silicon oxide (Fig. S1, ESI<sup>†</sup>) and most likely do not take part in the charge transport across the surrounding film whose general thickness decreases owing to the increasing local concentration of material in the above-mentioned aggregates. The formation of the latter type of films occurs at temperatures  $> 170$  °C (Fig. S2, ESI<sup>†</sup>) and starts within 10 min (Fig. S3, ESI<sup>†</sup>) as revealed by AFM. Unlike the monotonic increase in mobility with the annealing temperature measured in HMDS-treated devices, a very sharp increase of nearly 100-fold peaking at 200 °C with values approaching  $0.1 \text{ cm}^2 \text{ V}^{-1} \text{ s}^{-1}$  is measured when SiO<sub>2</sub> is treated with OTS (Fig. 3). To the best of our knowledge, this is the highest reported value of electron mobility for ICBA. In general, the devices featured an  $I_{\text{on}}/I_{\text{off}}$  ratio of  $10^3$ – $10^4$  and threshold voltages that are always positive with a tendency to shift towards zero with the increasing annealing temperature. The latter behavior was found to be more pronounced in the case of OTS-treated SiO<sub>2</sub> (see Fig. S6, ESI<sup>†</sup>). The above-mentioned

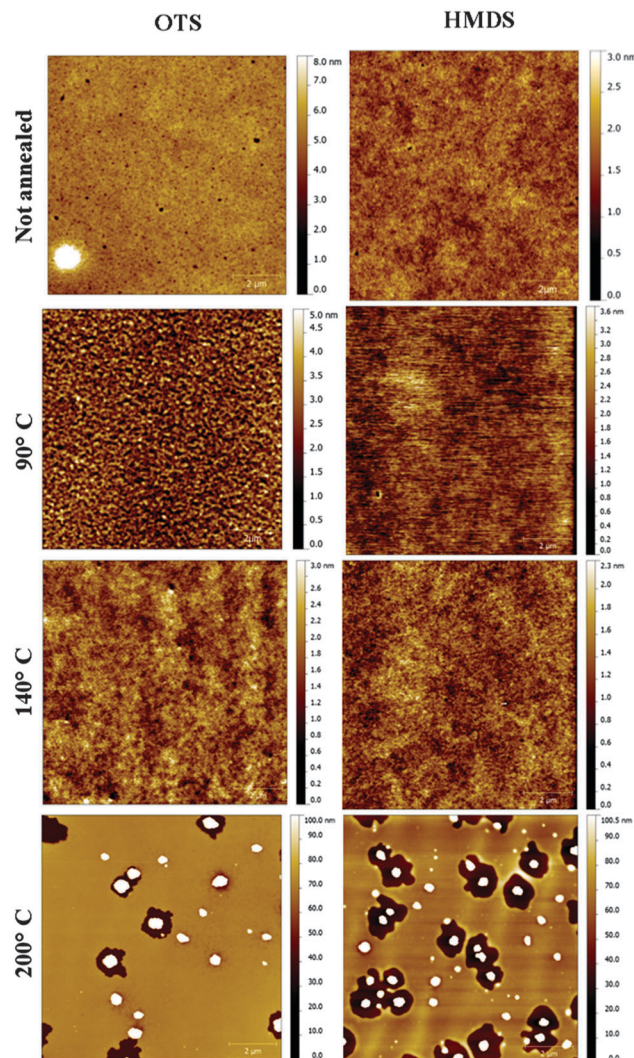


Fig. 2 Topographical atomic force microscopy images ( $10 \mu\text{m} \times 10 \mu\text{m}$ ) of spin-coated ICBA films ( $10 \text{ mg mL}^{-1}$  in chloroform) annealed at different temperature on either OTS or HMDS (annealing time: 1 h). For consistency with the device architecture, the imaged films are realized on a SiO<sub>2</sub> substrate.

threshold voltage shift is indicative of a film with improved crystallinity accompanied by a lower number of defects. In view of that, we put forward the hypothesis that the remarkable mobility increase, especially when OTS is used, stems from a peculiar thermodynamically-favorable assembly of the ICBA molecules which is, in addition, related to the annealing duration.

In order to better understand the relationship between structural order of the films and annealing temperature, grazing incidence X-ray diffraction (2D-GIXRD) measurements were performed by using synchrotron light radiation. The 2D-GIXRD measurements revealed that all films encompassed in this study have amorphous structure, regardless of the annealing temperature (see Fig. S7, ESI<sup>†</sup>) although an early stage of crystallization seems to appear upon annealing at 200 °C. To some extent, this behavior is unexpected if one compares ICBA to similar systems, such as PCBM, which is known to crystallize upon thermal annealing already at 150 °C.<sup>8</sup>



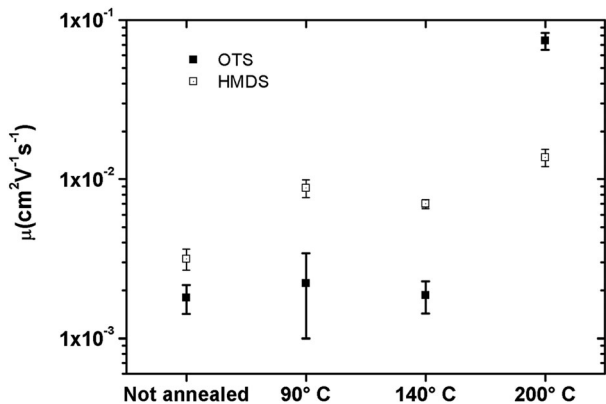


Fig. 3 The comparative plot displays the variation of field-effect saturation mobility for electrons in typical ICBA-based TFTs where the active layer underwent annealing at different temperatures. A different trend is recorded upon varying the functionalization of the SiO<sub>2</sub> surface with either OTS or HMDS. ( $W = 10$  mm,  $L = 2.5$  μm).

Noteworthy, not only thermodynamics rules the assembly and, consequently, the charge transport but the duration (kinetics) of the post-deposition assembly at the surface at a certain temperature was found to be a key parameter. Fig. 4 highlights the remarkable difference between 10 minutes, 1 hour and 4 days annealing time in the film's capacity to transport electrons. After 4 days of annealing, the morphology appeared to be characterized only by disconnected tall aggregates (Fig. S5, ESI<sup>†</sup>) without a continuous film around them bridging source and drain electrodes, therefore resulting in device currents close to the detection limit. The currents recorded after 1 h vs. 10 min annealing are indicative of a molecular assembly and morphology (*cf.* Fig. 2 and Fig. S3, ESI<sup>†</sup>) which promotes a better electron transport in the former case as confirmed by the large mobility variation  $\mu_{[1h]}/\mu_{[10min]} \sim 250$ .

In summary, we demonstrated that the electron transport within indene-C<sub>60</sub> bis-adduct (ICBA) thin films can be modified upon tuning the temperature and duration of thermal annealing post treatments as well as by treatment of the dielectric SiO<sub>2</sub> surface to

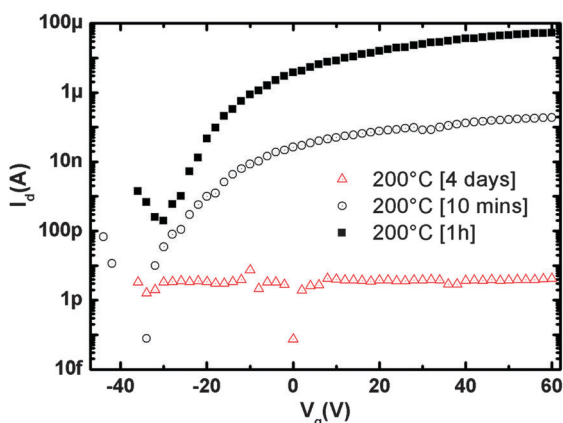


Fig. 4 Comparative transfer curves ( $I_d$ – $V_g$ ) of typical ICBA-based thin-film transistors with OTS-treated SiO<sub>2</sub> where the active layer underwent annealing at 200 °C for 4 days, 1 h or 10 minutes, respectively. ( $W = 10$  mm,  $L = 20$  μm;  $V_d = +60$  V).

render it hydrophobic. The electron mobility revealed a monotonic increase upon annealing for HMDS-treated SiO<sub>2</sub> whilst an abrupt enhancement was recorded at 200 °C on OTS-functionalized substrates. This difference can be correlated to a molecule–molecule interaction intimately entwined to molecule–substrate interaction owing to the type of surface treatment. ICBA molecules are freer to move and undergo self-assembly when supported on an OTS-treated SiO<sub>2</sub> by virtue of the lower surface energy they experience. By and large, the ability of promoting electron transport within the film at a given temperature has been found to depend on the particular kinetically-trapped phase in which the molecules are found in time. GIXRD did not provide strong evidence of structural order at the atomic scale. Hence, providing a more nuanced structural analysis with a different technique probing the aggregation at the nanoscale (such as grazing incidence small angle scattering) will be the subject of future work. The remarkable dependence of the charge transport upon the annealing duration and temperature as well as the surface energy is unambiguous evidence that ICBA transport properties strongly depend on the processing conditions. Besides its use as single component solution-processable n-type material for oTFTs, the ICBA appears to be a suitable candidate for replacing PCBM (in combination with P3HT) in oSC. Hence, these findings highlight how important and sensitive to the annealing temperature is the aggregation of the ICBA in determining its charge transport properties. This aspect can therefore be of high importance for unraveling the more complex materials' interplay which led to recent and promising results in terms of photovoltaic efficiency when using the ICBA as a replacement for PCBM in combination with P3HT.

This work was financially supported by the EC through the ERC project SUPRAFUNCTION (GA-257305), and the Marie Curie IEF project RESPONSIVE (PIEF-GA-2012-326665), the Agence Nationale de la Recherche through the LabEx project Chemistry of Complex Systems (ANR-10-LABX-0026\_CSC), and the International Center for Frontier Research in Chemistry (icFRC).

## Notes and references

- (a) M. Halik, H. Klauk, U. Zschieschang, G. Schmid, C. Dehm, M. Schutz, S. Maisch, F. Effenberger, M. Brunnbauer and F. Stellacci, *Nature*, 2004, **431**, 963–966; (b) H. Sirringhaus, *Adv. Mater.*, 2005, **17**, 2411–2425; (c) J. Zaumseil, C. L. Donley, J. S. Kim, R. H. Friend and H. Sirringhaus, *Adv. Mater.*, 2006, **18**, 2708–2712; (d) H. Klauk, U. Zschieschang, J. Pflaum and M. Halik, *Nature*, 2007, **445**, 745–748; (e) G. Dennler, M. C. Scharber and C. J. Brabec, *Adv. Mater.*, 2009, **21**, 1323–1338; (f) J. Rivnay, L. H. Jimison, J. E. Northrup, M. F. Toney, R. Noriega, S. F. Lu, T. J. Marks, A. Facchetti and A. Salleo, *Nat. Mater.*, 2009, **8**, 952–958; (g) H. Yan, Z. H. Chen, Y. Zheng, C. Newman, J. R. Quinn, F. Dötz, M. Kastler and A. Facchetti, *Nature*, 2009, **457**, 679–686; (h) A. C. Arias, J. D. MacKenzie, I. McCulloch, J. Rivnay and A. Salleo, *Chem. Rev.*, 2010, **110**, 3–24; (i) H. Klauk, *Chem. Soc. Rev.*, 2010, **39**, 2643–2666; (j) H. Sirringhaus, M. Bird, T. Richards and N. Zhao, *Adv. Mater.*, 2010, **22**, 3893–3898; (k) A. M. Lopez, A. Mateo-Alonso and M. Prato, *J. Mater. Chem.*, 2011, **21**, 1305–1318; (l) R. Noriega, J. Rivnay, K. Vandewal, F. P. V. Koch, N. Stingelin, P. Smith, M. F. Toney and A. Salleo, *Nat. Mater.*, 2013, **12**, 1037–1043; (m) A. Rao, P. C. Y. Chow, S. Gélinas, C. W. Schlenker, C. Z. Li, H. L. Yip, A. K. Y. Jen, D. S. Ginger and R. H. Friend, *Nature*, 2013, **500**, 435–439; (n) K. Vandewal, S. Albrecht, E. T. Hoke, K. R. Graham, J. Widmer, J. D. Douglas, M. Schubert, W. R. Mateker, J. T. Bloking, G. F. Burkhard, A. Sellinger, J. M. J. Fréchet, A. Amassian, M. K. Riede, M. D. McGehee, D. Neher and A. Salleo, *Nat. Mater.*, 2014, **13**, 63–68;



- (o) K. Vandewal, J. Widmer, T. Heumueller, C. J. Brabec, M. D. McGehee, K. Leo, M. Riede and A. Salleo, *Adv. Mater.*, 2014, **26**, 3839–3843.
- 2 (a) E. Voroshazi, K. Vasseur, T. Aernouts, P. Heremans, A. Baumann, C. Deibel, X. Xue, A. J. Herring, A. J. Athans, T. A. Lada, H. Richter and B. P. Rand, *J. Mater. Chem.*, 2011, **21**, 17345–17352; (b) E. T. Hoke, K. Vandewal, J. A. Bartelt, W. R. Mateker, J. D. Douglas, R. Noriega, K. R. Graham, J. M. J. Fréchet, A. Salleo and M. D. McGehee, *Adv. Energy Mater.*, 2013, **3**, 220–230; (c) S. Shoaee, S. Subramaniyan, H. Xin, C. Keiderling, P. S. Tuladhar, F. Jamieson, S. A. Jenekhe and J. R. Durrant, *Adv. Funct. Mater.*, 2013, **23**, 3286–3298; (d) X. Guo, M. J. Zhang, C. H. Cui, J. H. Hou and Y. F. Li, *ACS Appl. Mater. Interfaces*, 2014, **6**, 8190–8198.
- 3 (a) T. D. Anthopoulos, C. Tanase, S. Setayesh, E. J. Meijer, J. C. Hummelen, P. W. M. Blom and D. M. de Leeuw, *Adv. Mater.*, 2004, **16**, 2174–2179; (b) T. D. Anthopoulos, D. M. de Leeuw, E. Cantatore, P. van't Hof, J. Alma and J. C. Hummelen, *J. Appl. Phys.*, 2005, **98**, 054503; (c) H. Yu, H. H. Cho, C. H. Cho, K. H. Kim, D. Y. Kim, B. J. Kim and J. H. Oh, *ACS Appl. Mater. Interfaces*, 2013, **5**, 4865–4871.
- 4 (a) D. Bonifazi, O. Enger and F. Diederich, *Chem. Soc. Rev.*, 2007, **36**, 390–414; (b) C. Z. Li, C. C. Chueh, H. L. Yip, J. Y. Zou, W. C. Chen and A. K. Y. Jen, *J. Mater. Chem.*, 2012, **22**, 14976–14981; (c) A. M. Nardes, A. J. Ferguson, J. B. Whitaker, B. W. Larson, R. E. Larsen, K. Maturova, P. A. Graf, O. V. Boltalina, S. H. Strauss and N. Kopidakis, *Adv. Funct. Mater.*, 2012, **22**, 4115–4127.
- 5 J. M. Ball, R. K. M. Bouwer, F. B. Kooistra, J. M. Frost, Y. B. Qi, E. B. Domingo, J. Smith, D. M. de Leeuw, J. C. Hummelen, J. Nelson, A. Kahn, N. Stingelin, D. D. C. Bradley and T. D. Anthopoulos, *J. Appl. Phys.*, 2011, **110**, 014506.
- 6 Y. J. He, H. Y. Chen, J. H. Hou and Y. F. Li, *J. Am. Chem. Soc.*, 2010, **132**, 1377–1382.
- 7 S. Nilsson, A. Bernasik, A. Budkowski and E. Moons, *Macromolecules*, 2007, **40**, 8291–8301.
- 8 E. Verploegen, R. Mondal, C. J. Bettinger, S. Sok, M. F. Toney and Z. A. Bao, *Adv. Funct. Mater.*, 2010, **20**, 3519–3529.

